iScience

CellPress
OPEN ACCESS

Article

Chromatin target of protein arginine methyltransferases alleviates cerebral ischemia/reperfusion-induced injury by regulating RNA alternative splicing

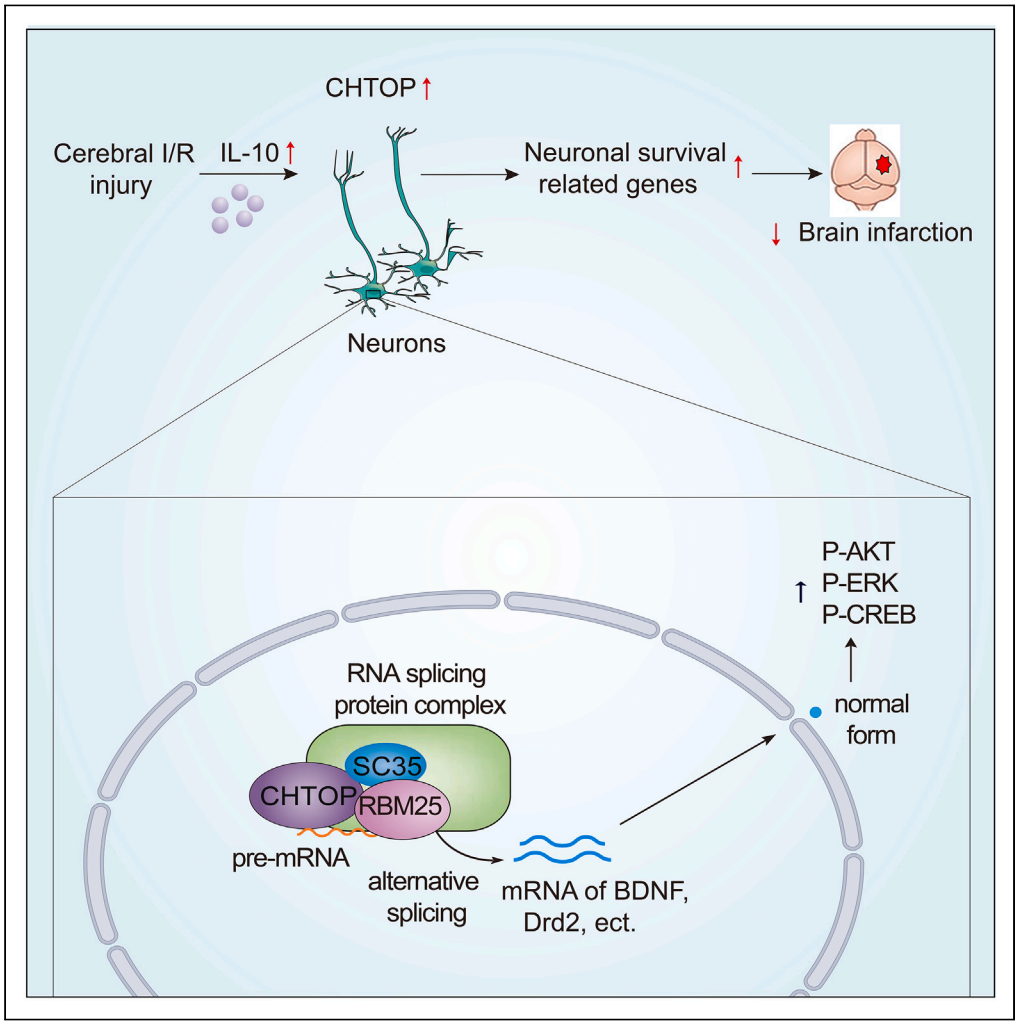

Yu Cui, Zhaolong Zhang, Mengfei Lv, ..., Jingchen Gao, Rui Xu, Qi Wan

cuiyu@qdu.edu.cn (Y.C.)
qiwan1@hotmail.com (Q.W.)

Highlights

RNA splicing in neurons alters early after OGD/R

CHTOP shows high expression in neurons, and IL-10 increases its expression after I/R

Nuclear speckle-localized CHTOP reduces neuronal death via regulating RNA splicing

IL-10 protects neurons against cell death by modulating CHTOP-mediated RNA splicing

Cui et al., iScience 27, 108688
January 19, 2024
https://doi.org/10.1016/j.isci.2023.108688

iScience

CellPress
OPEN ACCESS

Article

Chromatin target of protein arginine methyltransferases alleviates cerebral ischemia/reperfusion-induced injury by regulating RNA alternative splicing

Yu Cui,[1,2,4,*] Zhaolong Zhang,[3,4] Mengfei Lv,[1,2] Zhongying Duan,[1,2] Wenhao Liu,[3] Jingchen Gao,[1] Rui Xu,[3] and Qi Wan[1,2,5,*]

SUMMARY

RNA splicing is a post-transcriptional event that regulates many physiological and pathological events. However, whether RNA splicing regulates cerebral I/R-induced brain injury remains largely unknown. In this study, we found that the chromatin target of Prmts (CHTOP) was highly expressed in neurons, and anti-inflammatory cytokine interleukin-10 (IL-10) upregulates its expression after ischemia. In addition, overexpression or knockdown of CHTOP alleviated or exacerbated neuronal death in both experimental stroke mice and cultured neurons. Mechanistically, RNA alternative splicing is altered early after oxygen and glucose deprivation/reoxygenation (OGD/R). CHTOP interacted with nuclear speckle-related proteins to regulate alternative mRNA splicing of neuronal survival-related genes after OGD/R. In addition, I/R injury-induced cytokines IL-10 regulate CHTOP-mediated RNA splicing to alleviate ischemic brain injury. Taken together, this study reveals the alteration of RNA splicing after OGD/R and identifies the IL-10-CHTOP-RNA splicing axis as a modulator of brain injury, which may be promising therapeutic targets for ischemic stroke.

INTRODUCTION

Ischemic stroke is one of the most devastating neurological disorders and causes severe permanent disability. Tissue plasminogen activator thrombolysis and intra-arterial therapy are the only effective treatments for ischemic stroke. However, the therapies may further aggravate neuronal death owing to ischemia-reperfusion (I/R) injury.[1,2] Many biochemical and molecular events, including glutamate excitotoxicity, oxidative stress, apoptosis, and inflammation, have been identified to be involved in ischemic neuronal injury, which may be regulated at the transcriptional, post-transcriptional, and translational levels.[3–5] Despite progress in some preclinical studies, there are no clinically approved neuroprotective treatments.

Alternative splicing of pre-mRNA transcripts is one of the post-transcriptional processes that regulate gene expression and the corresponding biological events.[6] Splicing occurs through a dynamic ribonucleoprotein complex, the spliceosome.[7] In eukaryotes, splicing-related factors are involved in the development as well as the progression of some diseases, such as cancer, neurodegenerative diseases, and muscular dystrophies.[8–10] Cerebral I/R induces a variety of changes due to the lack of nutrients after ischemia and the recurrence of nutrients after reperfusion. Till now, whether RNA alternative splicing changes after cerebral I/R and I/R-released cytokines regulate I//R injury by modulating RNA splicing remains largely unknown, although some splicing-related factors have been reported to be involved in various I/R injuries.[11–13] Understanding these questions may provide important clues for the intervention of ischemic stroke by modulating RNA alternative splicing.

Glycine-arginine-rich (GAR) domains-containing proteins are involved in some physiological and pathological conditions by regulating gene transcription, translational repression, DNA damage signaling, and RNA splicing.[14] Chromatin target of Prmts (CHTOP) is a GAR domain–containing RNA-binding protein (RBP) that is believed to be a key contributor to RNA-protein interactions[14] and plays important roles in glioblastomagenesis,[15] cell apoptosis,[16] and proliferation.[17] CHTOP can both promote and repress specific gene transcription depending on which protein arginine methyltransferases (PRMTs) it recruits and the corresponding arginine methylation patterns.[18] In addition, as a component of the TREX (TRanscription-EXport) complex, CHTOP can bind RBPs and facilitate the translocation of mRNA from the nucleus to the cytoplasm.[18,19] The role of CHTOP in cerebral I/R injuries remains unknown.

[1]Institute of Neuroregeneration and Neurorehabilitation, Qingdao University, 308 Ningxia Road, Qingdao, Shandong 266071, China
[2]Qingdao Medical College, Qingdao University, Qingdao 266071, China
[3]Department of Interventional Radiology, The Affiliated Hospital of Qingdao University, 16 Jiangsu Road, Qingdao, Shandong 266000, China
[4]These authors contributed equally
[5]Lead contact
*Correspondence: cuiyu@qdu.edu.cn (Y.C.), qiwan1@hotmail.com (Q.W.)
https://doi.org/10.1016/j.isci.2023.108688

Ischemic stroke induces a robust inflammatory response, which is involved in the whole process of stroke pathogenesis and serves as a prime target for the development of stroke therapies.[5,20] Ischemic damage-induced sterile neuroinflammation is caused by the recognition of danger/damage-associated molecular patterns (DAMPs), such as ATP, HMGB1, and damaged DNA, by specific pattern-recognition receptors (PRRs), during which both innate immune cells and peripheral immune cells release various inflammatory cytokines and factors to modulate neuronal survival and activity.[5,21–23] Understanding the molecular mechanisms of these immune-related factors in regulating I/R-induced brain injury may provide important clues for the therapeutic interventions of acute ischemic stroke.

In this study, we aimed to study how RNA alternative splicing alters early after I/R and whether CHTOP regulates cerebral I/R injury by modulating RNA splicing, thus revealing whether CHTOP-mediated RNA splicing could be a potential therapeutic target for ischemic stroke.

RESULTS

Chromatin target of protein arginine methyltransferases shows high expression in neurons and anti-inflammatory cytokine interleukin-10 increases its expression after ischemia-reperfusion

To investigate the role of CHTOP in I/R-induced neuronal death, we examined the expression pattern of CHTOP in the normal brain. Interestingly, CHTOP exhibited high colocalization with NeuN, a neuron-specific marker, and low colocalization in microglia (Iba-1$^+$) and astrocytes (GFAP$^+$) (Figures 1A and 1B). Consistent with the tissue staining results, CHTOP was also observed to show high abundance in primary cultured cortical neurons and low expression in microglia and astrocytes (Figures 1C and S1A). Further MAP2 immunostaining results demonstrated the localization of CHTOP in the nucleus of neurons (Figure S1A). Thus, CHTOP was highly expressed in neurons and lowly expressed in microglia and astrocytes.

We then tested the expression of CHTOP after cerebral I/R. Of note, the expression of CHTOP was increased in the peri-infarct region, and no alteration in the contralateral regions was observed (Figures 1D and S1B). Immunofluorescent staining confirmed the increased expression of CHTOP in the peri-infarct region of NeuN$^+$ neurons (Figure 1E). However, the expression of CHTOP was not obviously altered after OGD exposure, an *in vitro* treatment that mimics the pathways associated with brain ischemia (Figures 1F and S1C). The different expression pattern prompted us to hypothesize that factors released from injured brains might induce CHTOP upregulation in *in vivo* conditions. As previous studies have reported that inflammatory cytokines released from microglia or peripherally infiltrated immune cells regulate neuronal death after I/R,[5,21] we wondered whether these cytokines could regulate neuronal death by regulating CHTOP expression. We chose the well-known cytokines IL-4, IL-6, and IL-10 to test this hypothesis. The addition of IL-10 could significantly increase CHTOP expression, whereas IL-4 and IL-6 treatment showed no significant changes (Figures 1G and S1D). In addition, intranasal administration of recombinant IL-10 increased the expression of CHTOP in the peri-infarct region after ischemia (Figure 1H). These data indicate that CHTOP was highly expressed in neurons and IL-10 upregulated CHTOP expression after I/R.

Chromatin target of protein arginine methyltransferases alleviates ischemia-reperfusion-induced brain injury

To test the effects of CHTOP on I/R injury in *in vivo* conditions, we either knocked down or overexpressed CHTOP by injecting neuron-specific adeno-associated virus (AAV) with the hSyn promoter, three weeks before tMCAO into the cortex, and then evaluated whether neuron-specific knockdown or overexpression of CHTOP altered ischemic brain injury (Figure 2A). Immunofluorescent staining and Western blot data verified the specificity and efficiency of the AAV infection (Figures 2B–2C and S2A–S2D).

Knockdown of CHTOP significantly increased brain infarct volume and decreased neurological functions (Figures 2D–2F). Moreover, long-term functional recovery was further determined by using the rotarod test. Consistent with the infarct volume, functional recovery after the knockdown of CHTOP was impaired as decreased time spent on a rotating bar was observed (Figure 2G). In addition, overexpression of CHTOP reduced brain infarct volume and improved neurological functions (Figures 2H–2J). Moreover, overexpression of CHTOP significantly improved long-term motor functions (Figure 2K). These data indicate that CHTOP alleviates I/R injury.

Chromatin target of protein arginine methyltransferases promotes neuronal survival after oxygen and glucose deprivation/reoxygenation

We then investigated whether CHTOP could directly regulate I/R-induced neuronal death by using the OGD/R system *in vitro*. We transfected primary cultured cortical neurons with lentivirus and tested cell viability. Lentivirus-mediated knockdown of CHTOP decreased cell viability based on CCK8 and LDH results, and the reduced neuronal survival could be restored by CHTOP overexpression, indicating the specificity of CHTOP knockdown (Figures 3A–3C and S3A). In addition, overexpression of CHTOP by using the lentivirus LV-CHTOP reduced OGD/R-induced neuronal death, compared to corresponding controls (Figures 3D–3F and S3B). Thus, CHTOP could alleviate neuronal death after OGD/R *in vitro*.

Chromatin target of protein arginine methyltransferases is enriched in the nuclear speckles and interacts with mRNA splicing factors after oxygen and glucose deprivation/reoxygenation

To investigate the molecular mechanism underlying CHTOP-mediated regulation of neuronal survival after OGD/R, we identified its binding protein by immunoprecipitation and mass spectrometry (Figure 4A). Gene Ontology (GO) analysis for biological function showed that the pulled nuclear proteins, which were screened from cellular components of GO term as CHTOP was specifically located in the nucleus, were most highly related to mRNA splicing (Figure 4B and Table S1).

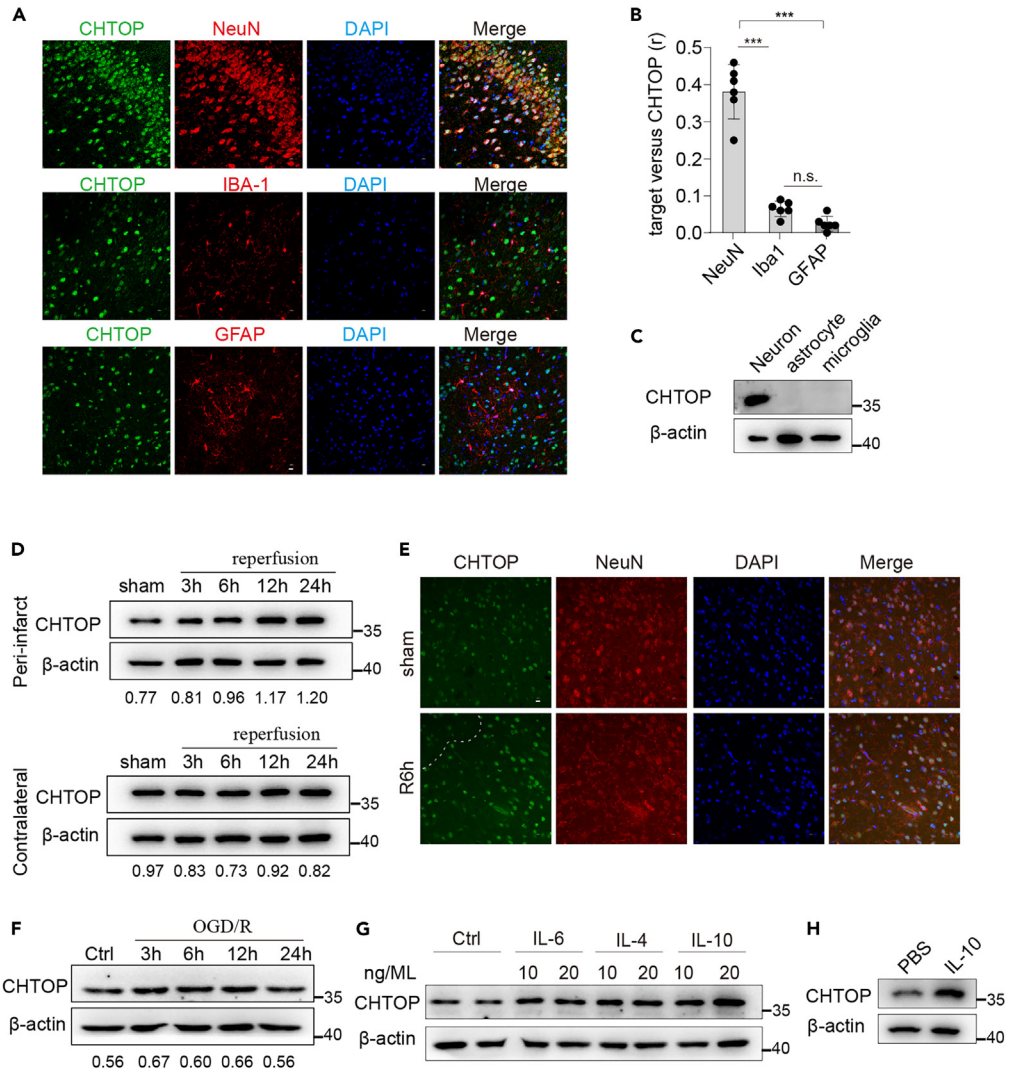

Figure 1. CHTOP shows high expression in neurons and IL-10 upregulates its expression after I/R

(A) Representative confocal images of CHTOP expression in cortex of C57BL/6 mice. Scale bar, 10 μm. n = 3 mice per group.

(B) Quantification of co-localization of NeuN, GFAP or Iba1 with CHTOP in normal conditions, calculated as Pearson's correlation coefficient, r. The data are means ± S.D. for all panels: ***$p < 0.001$, n.s., no significance. One-way ANOVA analysis was used followed by Turkey's test.

(C) Representative immunoblot of CHTOP expression in primary cultured neurons, microglia and astrocytes.

(D) Representative immunoblot and quantification of CHTOP in tissue extracts of mouse brains after 90 min tMCAO followed by various time points of reperfusion. β-actin served as a loading control. Numbers below lanes indicate densitometry of CHTOP relative to β-actin.

(E) Representative confocal images of CHTOP expression in cortex of C57BL/6 mice subjected to I/R for 6 h or under sham conditions. Scale bar, 10 μm.

(F) Representative immunoblot and quantification of CHTOP in primary cultured neurons after OGD followed by various time points of reoxygenation. β-actin served as a loading control. Numbers below lanes indicate densitometry of CHTOP relative to β-actin.

(G) Representative immunoblot of CHTOP expression in neurons treated with different concentrations of IL-4, IL-6 or IL-10 after reoxygenation for 6 h.

(H) Representative immunoblot of CHTOP expression in cortical brains injected with PBS or recombinant IL-10 for 48 h.

The selected nuclear speckle protein SF3B3 and RBM25, one nuclear speckle marker, showed significant enrichment with CHTOP in Neuro-2a cells after OGD/R (Figure 4C). Immunofluorescence assay of primary cortical neurons showed that nuclear CHTOP could co-localize with RBM25 and SC35, but failed to interact with SF3B3 in OGD/R conditions, which was observed in Neuro-2a cells (Figure 4D). As previous studies have shown the colocalization of CHTOP with Prmts, we further tested their interaction in OGD/R-treated neurons, and no obvious colocalization between CHTOP and Prmt1 was observed (Figure S4A). Moreover, CHTOP may not regulate the nuclear speckle organization as the intensity of nuclear speckle marker RBM25 did not alter after CHTOP knockdown in neurons (Figures 4E and S4B). Further analysis showed that knocking down CHTOP did not alter the expression of RBM25, SF3B3 and SC35

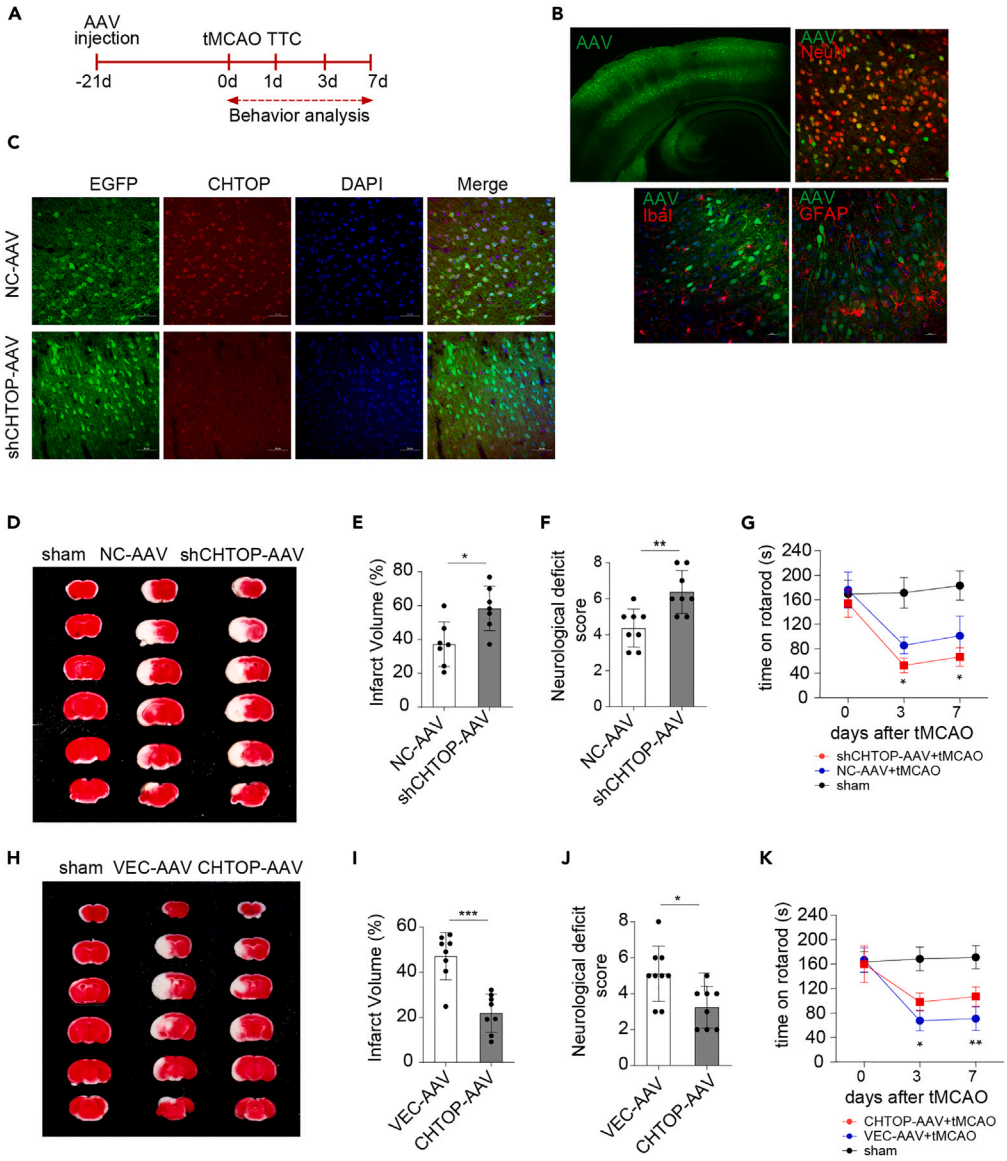

Figure 2. CHTOP protects mice against I/R injury

(A) Schematic of experimental timeline. AAV injected to the indicated sites in cortex at 21 days prior to tMCAO, and TTC staining was performed after 24 h. Rotarod test was assessed at baseline, 3 days or 7 days after tMCAO.

(B) Images represent expression of shNC-AAV in the cortex at 21 days post injection in naive tissue. shNC-AAV targets neurons. Viral EGFP expression (green) co-localizes with NeuN but does not co-localize with astrocytic marker, GFAP or microglial marker, IBA-1. Scale bar, 20 μm.

(C) Representative confocal images of CHTOP expression in NC-AAV-transfected or shCHTOP-AAV-transfected EGFP$^+$ neurons in the cortex of C57BL/6J mice. Scale bar, 50 μm. n = 3 mice per group.

(D) Representative brain slices stained by TTC at 24 h after tMCAO in sham, shNC-AAV or shCHTOP-AAV injected mice.

(E) Quantification of infarct volume at 24 h after tMCAO. n = 8 per group. The data are means ± S.D. *$p < 0.05$, Student's *t* test was used.

(F) Neurological severity score at 24 h after reperfusion. n = 8 for each group. The data are means ± S.D. **$p < 0.01$, Student's *t* test was used.

(G) Knockdown of CHTOP in neurons deteriorates long-term neurological deficits after tMCAO as assessed by rotarod tests. n = 7 for each group. The data are means ± S.D. *$p < 0.05$, two-way ANOVA analysis were used followed by Turkey's test.

(H) Representative brain slices stained by TTC at 24 h after tMCAO in sham, VEC-AAV or CHTOP-AAV injected mice.

(I) Quantification of infarct volume at 24 h after tMCAO. n = 8 per group. The data are means ± S.D. ***$p < 0.001$, Student's *t* test was used.

(J) Neurological severity score at 24 h after reperfusion. The data are means ± S.D. **$p < 0.01$, Student's *t* test was used.

(K) Overexpression of CHTOP in neurons alleviates long-term neurological deficits after tMCAO as assessed by rotarod tests. n = 7 for each group. The data are means ± S.D. *$p < 0.05$, two-way ANOVA analysis was used followed by Turkey's test.

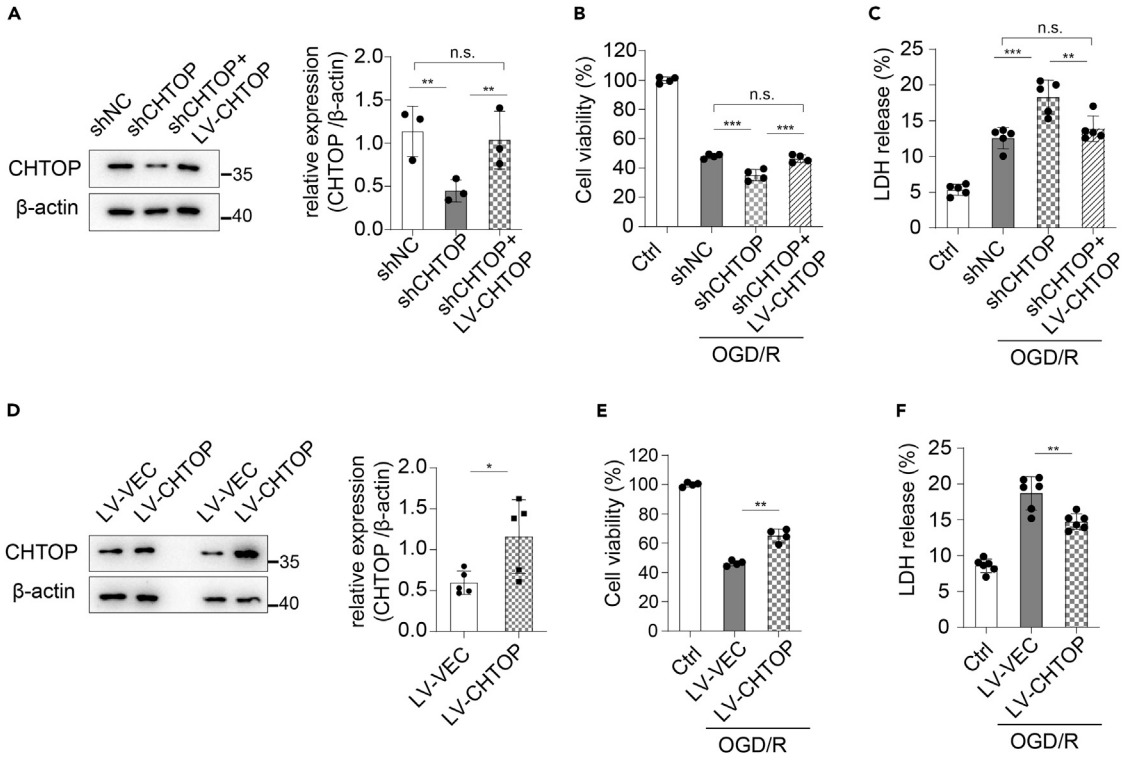

Figure 3. CHTOP promotes neuronal survival after OGD/R insult

(A, E) Representative immunoblot and quantification of CHTOP in neurons transfected with different lentiviruses for three days. β-actin served as a loading control. The data are means ± S.D. **p < 0.01, ***p < 0.001, n.s., no significance. One-way ANOVA analysis (A) was used followed by Turkey's test, Student's *t* test was used (E).

(B, D) Cell viability was assessed and quantified for transfected neurons subjected to OGD/R for 24 h or without treatment (Ctrl). The primary cultured neurons were transfected with different lentiviruses for 3 days before cell viability. The data are means ± S.D. **p < 0.01, ***p < 0.001, n.s., no significance. One-way ANOVA analysis was used followed by Turkey's test.

(C, F) LDH release was assessed and quantified for transfected neurons subjected to OGD/R for 24 h or without treatment (Ctrl). The primary cultured neurons were transfected with different lentiviruses for 3 days before LDH release assay. The data are means ± S.D. **p < 0.01, ***p < 0.001, n.s., no significance. One-way ANOVA analysis was used followed by Turkey's test.

(Figures 4F and S4C). These findings indicate that CHTOP could localize in the nuclear speckles by interacting with key nuclear speckle proteins after OGD/R.

RNA splicing profile alters in neurons early after oxygen and glucose deprivation/reoxygenation insult

Nuclear speckle is highly enriched with RNA processing factors and its function is predominantly linked to mRNA splicing. We wonder whether RNA splicing was altered early after OGD/R. To resolve this question, we cultured cortical neurons, subjected neurons to OGD/R treatment, and performed RNA sequencing (RNA-seq) as well as subsequent splicing analysis using rMATs software as described previously.[24,25] Notably, a total of 416 splicing events displayed significant changes in splicing patterns in OGD/R-treated neurons compared to the control (Table S2), wherein exon skipping was the most dominant event (43.75%); other splicing events included alternative 5'splice sites (17.79%), alternative 3'splice sites (14.66%), intron retention (12.98%), and mutually exclusive exon inclusions (10.82%) (Figures 5A and 5B). Thus, OGD/R treatment led to changes in multiple alternative splicing events in neurons.

KEGG pathway enrichment analysis of the genes involved in significant splicing changes showed that pathways relating to mRNA stability, cell metabolism, and synapse were enriched obviously (Figure 5C). We next verified the alternative splicing patterns of genes involved in mRNA surveillance, cell metabolism, and synapses, and observed decreased skipping over exon 4 of Dlgap, over exon 5 of Gabra2, significantly increased skipping over exon 6 of Drd2, over exon 2 of Rnps1, Lcmt, NcoR2, and Gmppa, and significantly increased 5′ alternative splicing over exon 6 of Cyb5r1 (Figures 5D–5F). Consistent with the splicing results, RNA-seq data of the OGD/R-treated neurons and control neurons showed that genes relating to cell metabolisms such as oxidative phosphorylation and propanoate pyruvate metabolism were significantly reduced, whereas genes relating to MAPK signaling and PI3K-Akt signaling were significantly induced early after OGD/R treatment (Figure S5A and S5B). Therefore, the altered gene expression profile early after OGD/R might have a relationship with the altered alternative splicing changes.

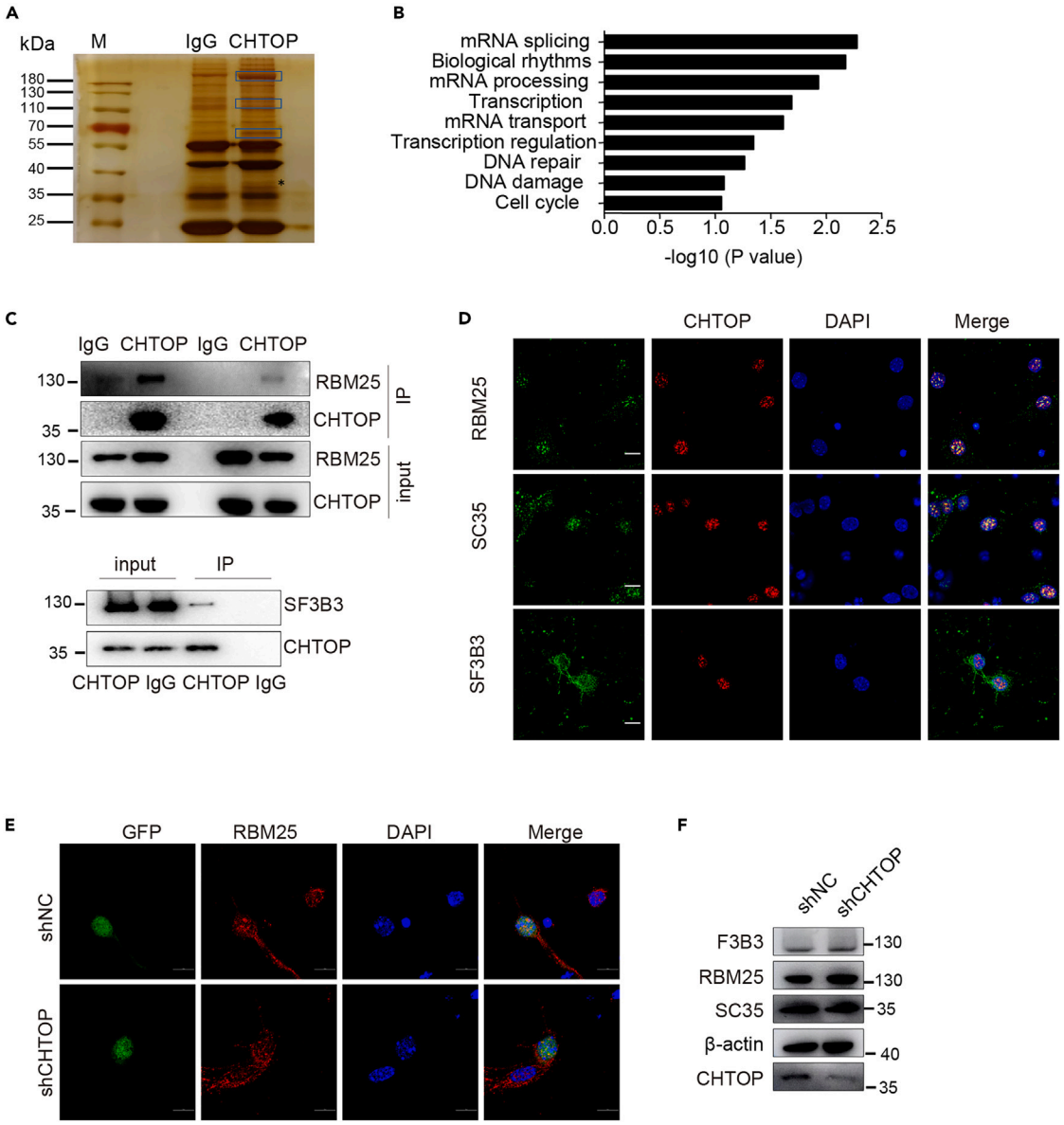

Figure 4. CHTOP is enriched in the nuclear speckles and interacts with mRNA splicing factors after OGD/R

(A) Representative gel used for MS analysis. The blue area was cut for MS analysis. Asterisk indicates CHTOP band.

(B) GO analysis of CHTOP-pulled nuclear proteins.

(C) Immunoblot analysis of RBM25, SF3B3 immunoprecipitated by CHTOP or IgG antibodies in N2a cells after OGD/R for 6 h treatment.

(D) Representative confocal images of the colocalization of CHTOP with RBM25, SC35 and SF3B3 in primary cultured neurons after OGD/R for 6 h treatment. Scale bar, 10 μm.

(E) Representative confocal images of the expression of RBM25 in shNC and shCHTOP-transfected neurons subjected to OGD/R6hr treatment. Scale bar, 10 μm.

(F) Representative immunoblot of SF3B3, RBM25, SC35 and CHTOP in neurons transfected with shNC or shCHTOP lentiviruses for three days and subjected to OGD/R treatment. β-actin served as a loading control.

Chromatin target of protein arginine methyltransferases regulates alternative RNA splicing to reduce neuronal death

A total of 195 splicing events displayed significant splicing pattern changes after comparison between CHTOP-knockdown neurons and control neurons early after OGD/R treatment. Among the altered splicing events, exon skipping was the most dominant event (Figures S6A, S6B, and Figure 6A; Table S3). Thus, CHTOP deficiency led to significant changes in multiple alternative splicing events, especially exon skipping.

Given that CHTOP facilitated neuronal survival after OGD/R, we postulated that CHTOP might regulate alternative splicing of genes involved in neuronal survival. Notably, cell cycle, terpenoid backbone biosynthesis, neurotrophin, and synapse-related pathways were significantly enriched based on KEGG pathway analysis (Figure 6B). Accordingly, genes related to the cell cycle, synapse, and neurotrophin

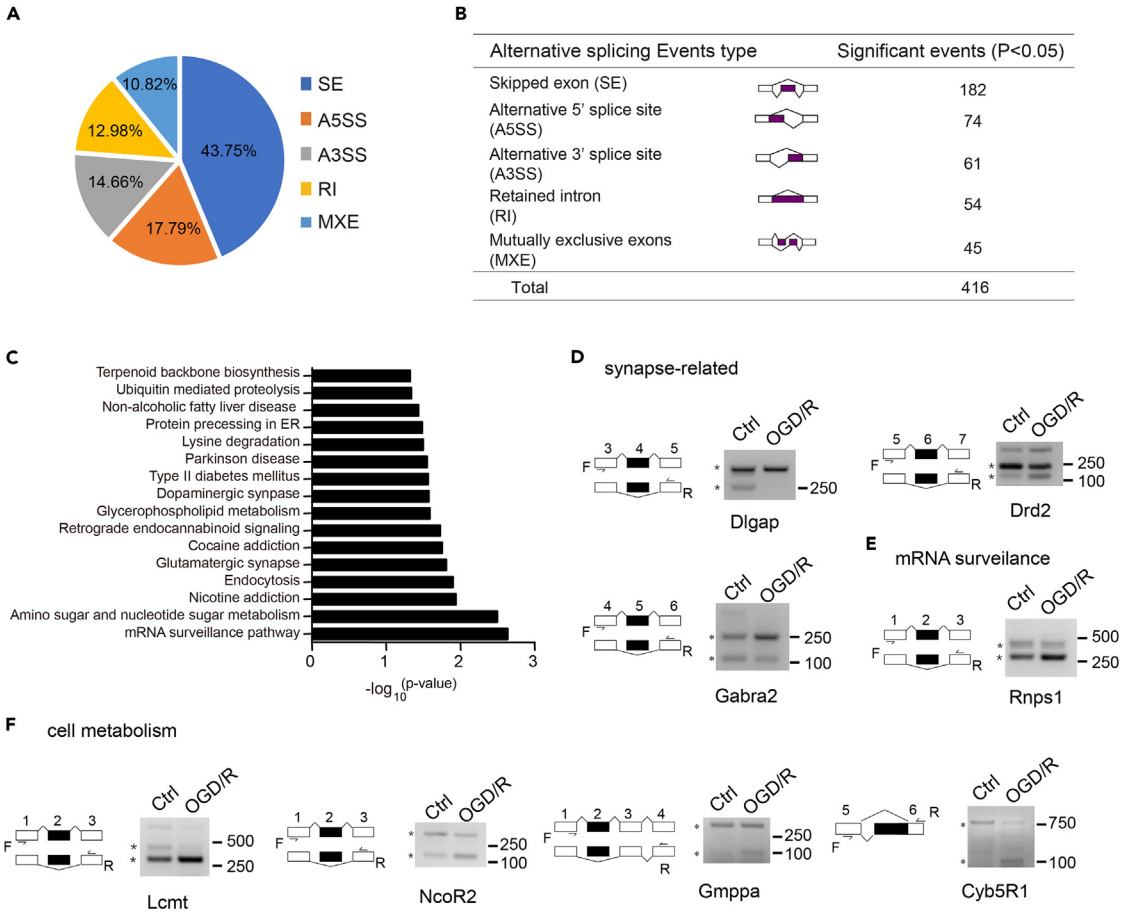

Figure 5. RNA splicing profile alters in neurons early after OGD/R insult

(A) Pie chart indicating the distribution of the differentially altered RNA splicing events including exon skipping (SE), intron retention (IR) and other splicing events such as alternative 5′ splice site (A5SS), alternative 3′ splice site(A3SS) and mutually exclusive exon (MXE) in cortical neurons in normal condition or after OGD/R6hr treatment.

(B) Number of significantly changed alternative splicing events in normal conditions or after OGD/R6hr treatment.

(C) KEGG pathway enrichment analysis of genes exhibiting altered RNA splicing in normal conditions or after OGD/R6hr treatment.

(D–F) Alternative splicing products of synapse-related genes (Dlgap, Drd2, and Gabra2) (D), mRNA surveillance (Rnps1) (E) and cell metabolism-related genes (Lcmt1, NcoR2, Gmppa, and Cyb5R1) (F) determined by qRT-PCR in the neurons of Ctrl or OGD/R6hr treatment. (n = 3). Asterisk indicates spliced variants, F and R denote primers used for qRT-PCR.

signaling pathways showed altered RNA splicing patterns. Significantly increased skipping over exon 12 of Cdc14b and exon 6 of Drd2, and no obvious skipping over exon 2 of NTF3 were observed (Figure 6C). In addition, 5′ alternative splicing of the BDNF gene occurred in the 5′-UTR sequence which might affect its translational efficiency and protein level (Figure 6C). Among them, we focused on BDNF, which has been well established as a neuroprotective factor both during development and after ischemia.[26–28] As RNA splicing finally regulates protein diversity or expression, we tested the protein expression level of BDNF. Knockdown of CHTOP reduced mature BDNF expression after OGD/R (Figure 6D). Accordingly, the downstream signaling pathway of BDNF, including phosphorylation of CREB, Akt, and ERK was also attenuated (Figure 6E). In addition, RNA immunoprecipitation (RIP) analysis confirmed the binding of CHTOP on BDNF 5′UTR regions after OGD/R (Figure 6F) and the mRNA of Drd2 and Cdc14b was also enriched by CHTOP (Figure S6C). Moreover, BDNF partially rescued the phenotype caused by CHTOP knockdown (Figure 6G). Therefore, CHTOP could bind the mRNA of cell survival related genes and regulate the alternative splicing of these genes to facilitate neuronal survival after OGD/R.

The surrounding cytokine interleukin-10 regulates Chromatin target of protein arginine methyltransferases-mediated RNA splicing axis to promote neuronal survival after ischemia-reperfusion

As IL-10 upregulated CHTOP expression, we wondered whether IL-10 modulated neuronal death by regulating CHTOP expression. The addition of IL-10 promoted neuronal viability either in normal conditions or after OGD/R treatment, whereas, no obvious difference was observed in neurons treated either with IL-4 or IL-6 (Figures 7A, 7B, S7A, S7B). More importantly, the presence of IL-10 ameliorated OGD/R-induced

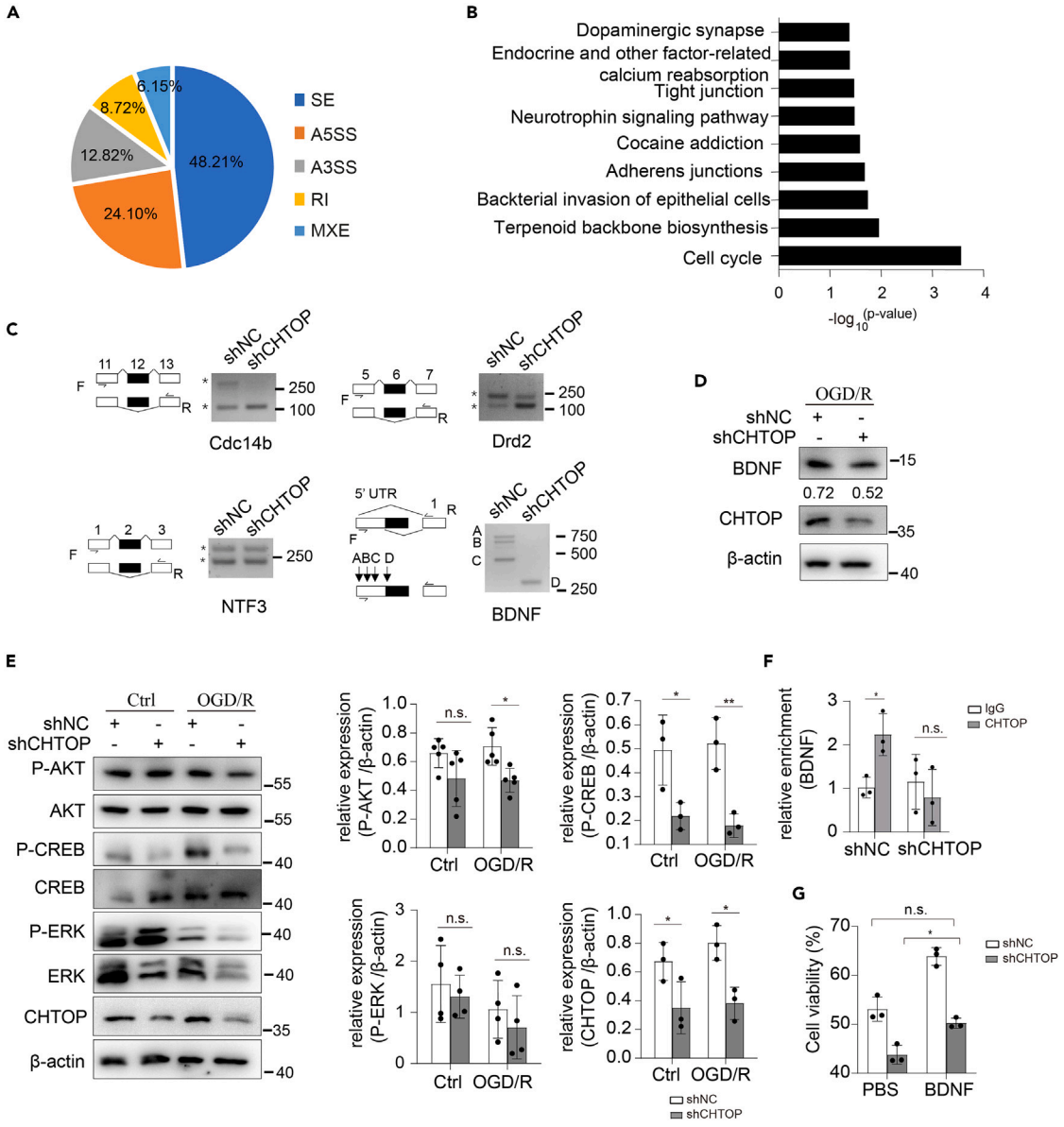

Figure 6. RNA splicing profile alters in neurons early after OGD/R insult

(A) Pie chart indicating the distribution of the differentially altered RNA splicing events including exon skipping (SE), intron retention (IR) and other splicing events such as alternative 5′ splice site (A5SS), alternative 3′ splice site(A3SS) and mutually exclusive exon (MXE) in shNC or shCHTOP-transfected cortical neurons after OGD/R6hr treatment.

(B) KEGG pathway enrichment analysis of genes exhibiting altered RNA splicing in shNC or shCHTOP-transfected cortical neurons after OGD/R6hr treatment.

(C) Alternative splicing products of Cdc14b, Drd2, NTF3 and BDNF determined by qRT-PCR in shNC or shCHTOP-transfected cortical neurons after OGD/R6hr treatment. (n = 3). Asterisk indicates spliced variants, F and R denote primers used for qRT-PCR.

(D) Representative immunoblot of CHTOP and BDNF expression in neurons transfected with shNC or shCHTOP lentivirus prior to OGD/R6hr treatment. β-actin served as a loading control.

(E) Representative immunoblot and quantification of P-AKT, AKT, P-CREB, CREB, P-ERK, ERK and CHTOP expression in neurons transfected with shNC or shCHTOP lentivirus for three days prior to OGD/R6hr treatment. The data are means ± S.D. for all panels: *p < 0.05, **p < 0.01, n.s., no significance. two-way ANOVA analysis were used followed by Bonferroni test.

(F) RIP qRT-PCR analysis of BDNF mRNAs in shNC or shCHTOP-transfected neurons after OGD/R treatemtnt by CHTOP or IgG enrichment. The data are means ± S.D. *p < 0.05, n.s., no significance. two-way ANOVA analysis were used followed by Sidak test.

(G) Cell viability was assessed and quantified for shNC or shCHTOP-transfected neurons subjected to OGD/R for 24 h in the presence of BDNF or PBS. The data are means ± S.D. for all panels: *p < 0.05, n.s., no significance. Two-way ANOVA analysis were used followed by Bonferroni test.

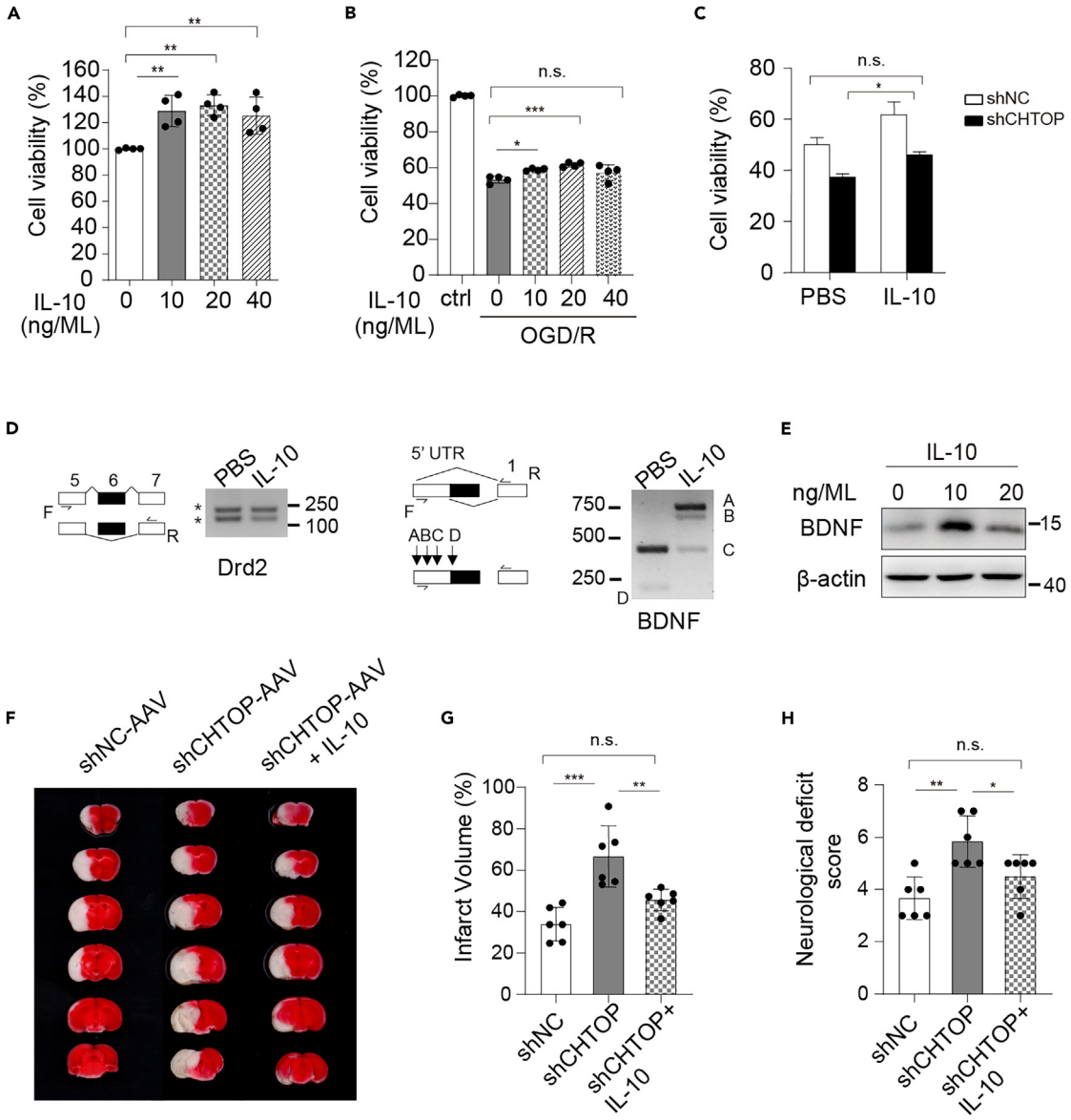

Figure 7. IL-10 regulates CHTOP-mediated RNA splicing to promote neuronal survival after I/R

(A, B) Cell viability was assessed and quantified for cortical neurons subjected to OGD/R for 24 h in the presence of different concentrations of IL-10. The data are means ± S.D. *p < 0.05, **p < 0.01, ***p < 0.001, n.s., no significance. One-way ANOVA analysis was used followed by Turkey's test.

(C) Cell viability was assessed and quantified for shNC or shCHTOP-transfected neurons subjected to OGD/R for 24 h in the presence of IL-10 or PBS. The data are means ± S.D. *p < 0.05, n.s., no significance. Two-way ANOVA analysis was used followed by Bonferroni test.

(D) Alternative splicing products of Drd2 and BDNF determined by qRT-PCR in PBS or IL-10-treated cortical neurons after OGD/R6hr treatment. (n = 3). Asterisk indicates spliced variants, F and R denote primers used for RT-PCR.

(E) Representative immunoblot of BDNF expression in neurons treated with different concentrations of IL-10 after reoxygenation for 6 h.

(F) Representative brain slices stained by TTC at 48 h after tMCAO in shNC-AAV, shCHTOP-AAV or shCHTOP-AAV plus IL-10-injected mice.

(G) Quantification of infarct volume at 48 h after tMCAO. n = 6 per group. The data are means ± S.D. for **p < 0.01, ***p < 0.001, n.s., no significance. One-way ANOVA analysis were used followed by Turkey's test.

(H) Neurological severity score at 48 h after reperfusion. The data are means ± S.D. for *p < 0.05, **p < 0.01, n.s., no significance. One-way ANOVA analysis were used followed by Turkey's test.

neuronal death after knockdown of CHTOP (Figure 7C). Thus, cytokine IL-10 might exert neuroprotective effects by increasing CHTOP expression.

We then tested whether IL-10 could also regulate CHTOP-mediated RNA splicing. The addition of IL-10 in primary neurons altered the splicing of some genes including Drd2 and BDNF (Figure 7D). Accordingly, the addition of IL-10 increased the protein level of BDNF in

neurons after OGD/R treatment (Figure 7E). Furthermore, *in vivo* administration of recombinant IL-10 attenuated infarct volume and neurological deficit score after knockdown of CHTOP (Figures 7F–7H). Collectively, IL-10 regulated CHTOP-mediated RNA splicing to modulate neuronal survival after cerebral I/R.

DISCUSSION

Many biochemical and molecular events regulated at the transcriptional, post-transcriptional, and translational levels contribute to ischemic neuronal injury. At present, no effective clinically approved neuroprotective treatments exist. As a post-transcriptional process, the role of alternative splicing in ischemic stroke is largely unknown. In this study, we reveal the alteration of RNA splicing after OGD/R, and identify IL-10-CHTOP-RNA splicing axis as modulators of brain injury after I/R injury, which may be promising therapeutic targets for ischemic stroke.

RNA alternative splicing is increasingly being recognized as an important layer of post-transcriptional gene expression and is involved in both development[29,30] and various kinds of diseases.[7,31–33] The milieu changes greatly after I/R. For example, many metabolites are accumulated[34,35] and various cytokines and chemokines are released.[5,21] How RNA splicing alters in response to these changing milieus after cerebral I/R is poorly understood, although some RNA splicing factors or other factors have been reported in certain ischemia models, such as brain ischemia,[11] heart ischemia,[36] kidney I/R[12] and hepatic ischemia.[13] Understanding how RNA splicing alters after cerebral I/R and exploring the underlying molecular mechanisms may provide an avenue for finding attractive therapeutic targets for ischemic stroke. In this study, we showed that RNA splicing changes greatly in the early phase after OGD/R, and genes involved in cell metabolism, synapses, and RNA surveillance exhibit obvious RNA splicing, which is consistent with RNA expression profiles (Figure 5). In addition, I/R-induced secretion of anti-inflammatory cytokine IL-10 could regulate RNA splicing to reduce neuronal death (Figure 6). Together with previous studies, these data demonstrate that RNA splicing is altered after organ I/R, and inflammatory cytokines could modulate RNA splicing to regulate neuronal survival. Thus, RNA splicing may be one potential layer of therapeutic intervention for ischemic stroke.

CHTOP has been reported to play important roles in glioblastomagenesis,[15] cell survival[16] and proliferation[17] by regulating gene transcription and RNA export. The role of CHTOP in cerebral I/R injury is unknown. In this study, we found that CHTOP upregulates its expression in the peri-infarct region after cerebral I/R injury (Figure 1). In addition, the effect of neuronal CHTOP on the outcome of ischemic stroke was explored using the neuron-specific CHTOP knockdown or overexpressed adeno-associated virus (Figure 2). Furthermore, we found that CHTOP is enriched in nuclear speckles and exhibits colocalization with splicing factors such as RBM25 and SC35 to regulate alternative splicing of some neuronal survival-related genes to further facilitate neuronal survival after brain injury (Figure 4). One previous study showed that CHTOP auto-regulates its expression level via intron retention and nonsense-mediated decay of its mRNA.[37] In addition, Maxim et al. demonstrated that Prmts can regulate the methylation of some RBPs including CHTOP and Sm to modulate retained introns.[38] Therefore, these studies demonstrate that CHTOP plays an important role in regulating RNA alternative splicing. Previous studies showed that GAR-domain containing proteins are involved in mediating the interaction of protein-protein and protein-RNAs via the GAR domain to promote the assembly of RNA-splicing related factors, which further potentiates RNA splicing.[39] In this study, we found that knockdown of CHTOP did not affect the expression of splicing factors and CHTOP could bind target RNA (Figures 4 and 6). Based on these data, two possible mechanisms of CHTOP in regulating RNA splicing can be proposed. Firstly, CHTOP may directly bind target RNA and recruit RNA splicing-related factors to promote RNA splicing; Secondly, CHTOP may promote the assemble of RNA-splicing networks and work as one member of the complex to regulate RNA splicing.

Therefore, modulating CHTOP expression may provide therapeutic interventions for acute ischemic stroke, although many interesting questions remain unresolved. For example, whether CHTOP is specifically expressed in neurons to regulate some processes during embryo development or CHTOP regulates neuronal activity as many synapses-related genes exhibit altered RNA splicing profiles. In addition, we showed that treatment with BDNF can partially rescue the reduced neuronal survival in CHTOP-knockdown neurons. How other downstream factors regulate CHTOP-mediated neuroprotection remains unknown.

I/R injury alters the brain environment and creates a milieu with immune-related factors, such as immune cells, proinflammatory cytokines, and anti-inflammatory cytokines.[5,21] Many previous studies have shown that immune-related factors regulate neuronal survival,[40] neurogenesis[41] or neuronal plasticity,[42] which further determine the outcome of I/R injury and long-term recovery of neurological function. However, the detailed molecular mechanisms are largely unknown. In this study, we showed that IL-10 can upregulate CHTOP expression and corresponding RNA splicing to promote neuronal survival (Figure 1). This is consistent with previous studies that IL-10 improves ischemic stroke outcomes,[43,44] and provides one potential mechanism of neuroprotection. In addition, the regulation of CHTOP by IL-10 may also explain why CHTOP is significantly increased in the penumbra after I/R, while the expression of CHTOP is not that obvious in cultured neurons subjected to OGD/R treatment (Figure 1). Moreover, it is possible that peripheral infiltrated immune cells or glial cell may also increase the expression of CHTOP which needs futher investigation. The molecular mechanism of other immune-related factors in regulating neuronal survival awaits more investigation and may hold potential to be a therapeutic target for modulating post-stroke neuronal survival and regeneration.

In conclusion, our findings indicate that OGD/R induces RNA splicing changes; I/R-induced cytokines IL-10 can modulate neuronal CHTOP-RNA splicing axis to facilitate neuronal survival. Thus, the IL-10-CHTOP-RNA splicing axis may serve as potential therapeutic target for ischemic stroke.

Limitation of the study

A limitation of the study is that we used neuron-specific adeno-associated virus (AAV) with hSyn promoter instead of CHTOP conditional knockout mice to demonstrate the *in vivo* role of this protein. As the transfection efficiency is relatively high, we can still draw the conclusion. In addition,

when mapping the RNA splicing changes we used 6 h after reoxygenation as a time point instead of picking more time points. As long-time treatment leads to severe neuronal death and our main aim is to recover the early changes of RNA splicing leading to neuronal death, we chose 6 h as a final time-point. How RNA splicing is dynamically changed during the whole process of reoxygenation still needs further investigation.

STAR★METHODS

Detailed methods are provided in the online version of this paper and include the following:

- KEY RESOURCES TABLE
- RESOURCE AVAILABILITY
  - Lead contact
  - Materials avialibity
  - Data and code availability
- EXPERIMENTAL MODEL AND STUDY PARTICIPANT DETAILS
  - Animals
  - Cell culture
- METHOD DETAILS
  - Focal cerebral ischemia
  - TTC staining and neurological severity score analysis
  - Brain tissue sample preparation
  - RNA immunoprecipitation (RIP)
  - Neuron viability assays
  - RNA extraction, reverse transcription and PCR for splicing analysis
  - OGD treatment
  - Lentivirus *in vitro* infection methods
  - Adeno-associated virus (AAV) *in vivo* administration methods
  - Behavior analysis
  - Immunoblot, Immunoprecipitation (IP) and Mass Spectrometry
  - Immunofluorescence
  - RNA sequencing and data analysis
- QUANTIFICATION AND STATISTICAL ANALYSIS
  - Statistical analysis

SUPPLEMENTAL INFORMATION

Supplemental information can be found online at https://doi.org/10.1016/j.isci.2023.108688.

ACKNOWLEDGMENTS

The authors wish to thank Dr. Shengli Gao from the Biomedical Center of Qingdao University for the use of some instruments and assistance with the measurements. This work was supported by Science and Technology Support Plan for Youth Innovation of Colleges and Universities of Shandong Province of China (2022KJ146) to Yu Cui; National Natural Science Foundation of China (82071385) to Qi Wan; National Natural Science Foundation of China (82101380), Natural Science Foundation of Shandong Province (ZR202102280316) and Postdoctoral Applied Research Project of Qingdao (QDBSH20220201049) to Zhaolong Zhang.

AUTHOR CONTRIBUTIONS

Y.C. designed and performed most experiments, designed the research, and prepared the article; Z.Z. performed all the MCAO, analyzed data and prepared the article; M.L. and Z.D. helped with the WB and RNA splicing experiments; W. L. and J. G. helped with WB and IF experiments; R. X. helped with data analysis and revised the article; Q.W. conceptualized the research, directed the study, and prepared the article.

DECLARATION OF INTERESTS

The authors declare no competing financial interests.

Received: August 22, 2023
Revised: November 1, 2023
Accepted: December 5, 2023
Published: December 7, 2023

REFERENCES

1. Berkhemer, O.A., Fransen, P.S.S., Beumer, D., van den Berg, L.A., Lingsma, H.F., Yoo, A.J., Schonewille, W.J., Vos, J.A., Nederkoorn, P.J., Wermer, M.J.H., et al. (2015). A randomized trial of intraarterial treatment for acute ischemic stroke. N. Engl. J. Med. *372*, 11–20.
2. Mizuma, A., You, J.S., and Yenari, M.A. (2018). Targeting Reperfusion Injury in the Age of Mechanical Thrombectomy. Stroke *49*, 1796–1802.
3. Chokkalla, A.K., Mehta, S.L., Kim, T., Chelluboina, B., Kim, J., and Vemuganti, R. (2019). Transient Focal Ischemia Significantly Alters the m(6)A Epitranscriptomic Tagging of RNAs in the Brain. Stroke *50*, 2912–2921.
4. Kiebler, M.A., Scheiffele, P., and Ule, J. (2013). What, where, and when: the importance of post-transcriptional regulation in the brain. Front. Neurosci. *7*, 192.
5. Zhang, Z., Lv, M., Zhou, X., and Cui, Y. (2022). Roles of peripheral immune cells in the recovery of neurological function after ischemic stroke. Front. Cell. Neurosci. *16*, 1013905.
6. Han, J., Xiong, J., Wang, D., and Fu, X.D. (2011). Pre-mRNA splicing: where and when in the nucleus. Trends Cell Biol. *21*, 336–343.
7. Lee, Y., and Rio, D.C. (2015). Mechanisms and Regulation of Alternative Pre-mRNA Splicing. Annu. Rev. Biochem. *84*, 291–323.
8. Baralle, M., and Baralle, F.E. (2021). Alternative splicing and liver disease. Ann. Hepatol. *26*, 100534.
9. Montes, M., Sanford, B.L., Comiskey, D.F., and Chandler, D.S. (2019). RNA Splicing and Disease: Animal Models to Therapies. Trends Genet. *35*, 68–87.
10. Baralle, F.E., and Giudice, J. (2017). Alternative splicing as a regulator of development and tissue identity. Nat. Rev. Mol. Cell Biol. *18*, 437–451.
11. Qi, Y., Li, Y., Cui, S.C., Zhao, J.J., Liu, X.Y., Ji, C.X., Sun, F.Y., Xu, P., and Chen, X.H. (2015). Splicing factor NSSR1 reduces neuronal injury after mouse transient global cerebral ischemia. Glia *63*, 826–845.
12. Lin, F., Xu, L., Yuan, R., Han, S., Xie, J., Jiang, K., Li, B., Yu, W., Rao, T., Zhou, X., and Cheng, F. (2022). Identification of inflammatory response and alternative splicing in acute kidney injury and experimental verification of the involvement of RNA-binding protein RBFOX1 in this disease. Int. J. Mol. Med. *49*, 32.
13. Dery, K.J., Kojima, H., Kageyama, S., Kadono, K., Hirao, H., Cheng, B., Zhai, Y., Farmer, D.G., Kaldas, F.M., Yuan, X., et al. (2023). Alternative splicing of CEACAM1 by hypoxia-inducible factor-1alpha enhances tolerance to hepatic ischemia in mice and humans. Sci. Transl. Med. *15*, eadf2059.
14. Thandapani, P., O'Connor, T.R., Bailey, T.L., and Richard, S. (2013). Defining the RGG/RG motif. Mol. Cell *50*, 613–623.
15. Takai, H., Masuda, K., Sato, T., Sakaguchi, Y., Suzuki, T., Suzuki, T., Koyama-Nasu, R., Nasu-Nishimura, Y., Katou, Y., Ogawa, H., et al. (2014). 5-Hydroxymethylcytosine plays a critical role in glioblastomagenesis by recruiting the CHTOP-methylosome complex. Cell Rep. *9*, 48–60.
16. Feng, X., Bai, X., Ni, J., Wasinger, V.C., Beretov, J., Zhu, Y., Graham, P., and Li, Y. (2019). CHTOP in Chemoresistant Epithelial Ovarian Cancer: A Novel and Potential Therapeutic Target. Front. Oncol. *9*, 557.
17. Zullo, A.J., Michaud, M., Zhang, W., and Grusby, M.J. (2009). Identification of the small protein rich in arginine and glycine (SRAG): a newly identified nucleolar protein that can regulate cell proliferation. J. Biol. Chem. *284*, 12504–12511.
18. Izumikawa, K., Ishikawa, H., Simpson, R.J., and Takahashi, N. (2018). Modulating the expression of Chtop, a versatile regulator of gene-specific transcription and mRNA export. RNA Biol. *15*, 849–855.
19. Chang, C.T., Hautbergue, G.M., Walsh, M.J., Viphakone, N., van Dijk, T.B., Philipsen, S., and Wilson, S.A. (2013). Chtop is a component of the dynamic TREX mRNA export complex. EMBO J. *32*, 473–486.
20. Shi, K., Tian, D.C., Li, Z.G., Ducruet, A.F., Lawton, M.T., and Shi, F.D. (2019). Global brain inflammation in stroke. Lancet Neurol. *18*, 1058–1066.
21. Jayaraj, R.L., Azimullah, S., Beiram, R., Jalal, F.Y., and Rosenberg, G.A. (2019). Neuroinflammation: friend and foe for ischemic stroke. J. Neuroinflammation *16*, 142.
22. Zhang, Z., Duan, Z., and Cui, Y. (2023). $CD8^+$ T cells in brain injury and neurodegeneration. Front. Cell. Neurosci. *17*, 1273459.
23. Lv, M., Zhang, Z., and Cui, Y. (2023). Unconventional T cells in brain homeostasis, injury and neurodegeneration. Front. Immunol. *14*, 1273459.
24. Zhang, Q., Zhang, J., Ye, J., Li, X., Liu, H., Ma, X., Wang, C., He, K., Zhang, W., Yuan, J., et al. (2021). Nuclear speckle specific hnRNP D-like prevents age- and AD-related cognitive decline by modulating RNA splicing. Mol. Neurodegener. *16*, 66.
25. Shen, S., Park, J.W., Lu, Z.X., Lin, L., Henry, M.D., Wu, Y.N., Zhou, Q., and Xing, Y. (2014). rMATS: robust and flexible detection of differential alternative splicing from replicate RNA-Seq data. Proc. Natl. Acad. Sci. USA *111*, E5593–E5601.
26. Koroleva, E.S., Brazovskaya, N.G., Levchuk, L.A., Kazakov, S.D., Romadina, N.Y., and Alifirova, V.M. (2020). [Assessment of the levels of neuron-specific enolase and BDNF at the stages of rehabilitation in the acute and early recovery periods of ischemic stroke]. Z. nevrol. psikhiatr. im. S. S. Korsakova *120*, 30–36.
27. Schäbitz, W.R., Sommer, C., Zoder, W., Kiessling, M., Schwaninger, M., and Schwab, S. (2000). Intravenous brain-derived neurotrophic factor reduces infarct size and counterregulates Bax and Bcl-2 expression after temporary focal cerebral ischemia. Stroke *31*, 2212–2217.
28. Bath, K.G., Akins, M.R., and Lee, F.S. (2012). BDNF control of adult SVZ neurogenesis. Dev. Psychobiol. *54*, 578–589.
29. Song, H., Wang, L., Chen, D., and Li, F. (2020). The Function of Pre-mRNA Alternative Splicing in Mammal Spermatogenesis. Int. J. Biol. Sci. *16*, 38–48.
30. Su, C.H., D, D., and Tarn, W.Y. (2018). Alternative Splicing in Neurogenesis and Brain Development. Front. Mol. Biosci. *5*, 12.
31. Chow, L.T., Gelinas, R.E., Broker, T.R., and Roberts, R.J. (1977). An amazing sequence arrangement at the 5' ends of adenovirus 2 messenger RNA. Cell *12*, 1–8.
32. Chen, H.C., and Cheng, S.C. (2012). Functional roles of protein splicing factors. Biosci. Rep. *32*, 345–359.
33. Wang, E., and Aifantis, I. (2020). RNA Splicing and Cancer. Trends Cancer *6*, 631–644.
34. Chumachenko, M.S., Waseem, T.V., and Fedorovich, S.V. (2022). Metabolomics and metabolites in ischemic stroke. Rev. Neurosci. *33*, 181–205.
35. Wang, X., Zhang, L., Sun, W., Pei, L.L., Tian, M., Liang, J., Liu, X., Zhang, R., Fang, H., Wu, J., et al. (2020). Changes of Metabolites in Acute Ischemic Stroke and Its Subtypes. Front. Neurosci. *14*, 580929.
36. Kong, S.W., Hu, Y.W., Ho, J.W.K., Ikeda, S., Polster, S., John, R., Hall, J.L., Bisping, E., Pieske, B., dos Remedios, C.G., and Pu, W.T. (2010). Heart failure-associated changes in RNA splicing of sarcomere genes. Circ. Cardiovasc. Genet. *3*, 138–146.
37. Izumikawa, K., Yoshikawa, H., Ishikawa, H., Nobe, Y., Yamauchi, Y., Philipsen, S., Simpson, R.J., Isobe, T., and Takahashi, N. (2016). Chtop (Chromatin target of Prmt1) auto-regulates its expression level via intron retention and nonsense-mediated decay of its own mRNA. Nucleic Acids Res. *44*, 9847–9859.
38. Maron, M.I., Casill, A.D., Gupta, V., Roth, J.S., Sidoli, S., Query, C.C., Gamble, M.J., and Shechter, D. (2022). Type I and II PRMTs inversely regulate post-transcriptional intron detention through Sm and CHTOP methylation. Elife *11*, e72867.
39. Godin, K.S., and Varani, G. (2007). How arginine-rich domains coordinate mRNA maturation events. RNA Biol. *4*, 69–75.
40. Lin, Y., Zhang, J.C., Yao, C.Y., Wu, Y., Abdelgawad, A.F., Yao, S.L., and Yuan, S.Y. (2016). Critical role of astrocytic interleukin-17 A in post-stroke survival and neuronal differentiation of neural precursor cells in adult mice. Cell Death Dis. *7*, e2273.
41. Meng, C., Zhang, J.C., Shi, R.L., Zhang, S.H., and Yuan, S.Y. (2015). Inhibition of interleukin-6 abolishes the promoting effects of pair housing on post-stroke neurogenesis. Neuroscience *307*, 160–170.
42. Liu, X., Liu, J., Zhao, S., Zhang, H., Cai, W., Cai, M., Ji, X., Leak, R.K., Gao, Y., Chen, J., and Hu, X. (2016). Interleukin-4 Is Essential for Microglia/Macrophage M2 Polarization and Long-Term Recovery After Cerebral Ischemia. Stroke *47*, 498–504.
43. Piepke, M., Clausen, B.H., Ludewig, P., Vienhues, J.H., Bedke, T., Javidi, E., Rissiek, B., Jank, L., Brockmann, L., Sandrock, I., et al. (2021). Interleukin-10 improves stroke outcome by controlling the detrimental Interleukin-17A response. J. Neuroinflammation *18*, 265.
44. Sun, W., Wang, S., and Nan, S. (2021). The Prognostic Determinant of Interleukin-10 in Patients with Acute Ischemic Stroke: An Analysis from the Perspective of Disease Management. Dis. Markers *2021*, 6423244.
45. Cui, Y., Zhang, Y., Zhao, X., Shao, L., Liu, G., Sun, C., Xu, R., and Zhang, Z. (2021). ACSL4 exacerbates ischemic stroke by promoting ferroptosis-induced brain injury and neuroinflammation. Brain Behav. Immun. *93*, 312–321.
46. Shao, W., Zhang, S.Z., Tang, M., Zhang, X.H., Zhou, Z., Yin, Y.Q., Zhou, Q.B., Huang, Y.Y., Liu, Y.J., Wawrousek, E., et al. (2013). Suppression of neuroinflammation by

astrocytic dopamine D2 receptors via alphaB-crystallin. Nature *494*, 90–94.

47. Lananna, B.V., McKee, C.A., King, M.W., Del-Aguila, J.L., Dimitry, J.M., Farias, F.H.G., Nadarajah, C.J., Xiong, D.D., Guo, C., Cammack, A.J., et al. (2020). Chi3l1/YKL-40 is controlled by the astrocyte circadian clock and regulates neuroinflammation and Alzheimer's disease pathogenesis. Sci. Transl. Med. *12*, eaax3519.
48. Swanson, R.A., Morton, M.T., Tsao-Wu, G., Savalos, R.A., Davidson, C., and Sharp, F.R. (1990). A semiautomated method for measuring brain infarct volume. J. Cereb. Blood Flow Metab. *10*, 290–293.
49. Dennis, G., Jr., Sherman, B.T., Hosack, D.A., Yang, J., Gao, W., Lane, H.C., and Lempicki, R.A. (2003). DAVID: Database for Annotation, Visualization, and Integrated Discovery. Genome Biol. *4*, P3.

STAR★METHODS

KEY RESOURCES TABLE

REAGENT or RESOURCE	SOURCE	IDENTIFIER
Antibodies		
Rabbit CHTOP antibody	Abcam	Cat# ab222861;RRID:AB_3073765
Rabbit polyclonal antibody	ThermoFisher Scientific	Cat# PA5-44307;RRID: AB_2576376
Phospho-Akt (Ser473) (D9E) XP® Rabbit mAb	Cell Signaling Technology	Cat# 4060S;RRID: AB_2315049
Akt antibody	Cell Signaling Technology	Cat# 9272; RRID: AB_329827
Phospho-CREB (Ser133) (87G3) Rabbit mAb	Cell Signaling Technology	Cat# 9198S; RRID: AB_2561044
CREB (86B10) Mouse mAb	Cell Signaling Technology	Cat# 9104S; RRID: AB_490881
Phospho-p44/42 MAPK (Erk1/2) (Thr202/Tyr204) Antibody	Cell Signaling Technology	Cat# 9101S; RRID: AB_331646
p44/42 MAPK (Erk1/2) (137F5) Rabbit mAb	Cell Signaling Technology	Cat# 4695; RRID: AB_390779
Beta Actin Monoclonal antibody	Proteintech	Cat# 66009-1-Ig; RRID: AB_2687938
HRP-conjugated Affinipure Goat Anti-Mouse IgG(H+L)	Proteintech	Cat# SA00001-1; RRID: AB_2722565
HRP-conjugated Affinipure Goat Anti-Rabbit IgG (H+L)	Proteintech	Cat# SA00001-2; RRID: AB_2722564
Mouse RBM25 antibody (H-4)	Santa Cruze technology	Cat# sc-374271; RRID: AB_10989549
Anti-SC35 antibody	Abcam	Cat# ab11826; RRID: AB_298608
SF3B3 Polyclonal antibody	Proteintech	Cat# 14577-1-AP; RRID: AB_2270189
Mouse prmt1 antibody	Santa Cruze technology	Cat# sc-166963; RRID: AB_10610884
Mouse MAP2 antibody	MERCK	Cat# M4403; RRID: AB_477193
BDNF antibody (ERP1292)	Abcam	Cat# 108319; RRID: AB_10862052
Donkey anti-rabbit 488	ThermoFisher Scientific	Cat# A-21206; RRID: AB_2535792
Donkey anti-mouse 568	ThermoFisher Scientific	Cat# A-10037; RRID: AB_2534013
Donkey anti-goat 568	ThermoFisher Scientific	Cat# A11057; RRID: AB_2534104
mouse GFAP antibody	MERCK	Cat# MAB360; RRID: AB_11212597
anti-NeuN clone A60 mouse	MERCK	Cat# MAB377; RRID: AB_2298772
Goat AIF-1/Iba1 Antibody	Novus	Cat# NB100-1028; RRID: AB_521594
Bacterial and virus strains		
pAAV-hSyn-EGFP-3xFLAG-miR30shRNA (Chtop)-WPRE	This paper (Obio Technology Corp., Ltd)	N/A
pAAV-hSyn-EGFP-3xFLAG-miR30shRNA(NC)-WPRE	This paper (Obio Technology Corp., Ltd)	N/A
pAAV-hSyn-EGFP-P2A-3xFLAG-WPRE	This paper (Obio Technology Corp., Ltd)	N/A
pAAV-hSyn-EGFP-P2A-Chtop-3xFLAG-WPRE	This paper (Obio Technolo)	N/A
Ubi-MCS-3FLAG-CBh-gcGFP-IRES -puromycin (lentivirus)	This paper (GeneChem Technology)	N/A
Ubi-MCS-chtop-3FLAG-CBh-gcGFP-IRES -puromycin (lentivirus)	This paper (GeneChem Technology)	N/A
LV3 (H1/GFP&puromcin) lentivirus	This paper (Genepharma Technology)	N/A
LV3-shCHTOP (H1/GFP&puromcin) lentivirus	This paper (Genepharma Technology)	N/A

(*Continued on next page*)

Continued

REAGENT or RESOURCE	SOURCE	IDENTIFIER
Chemicals, peptides, and recombinant proteins		
Recombinant murine IL-4	Peprotech	Cat# 214-14
Recombinant murine IL-6	Peprotech	Cat# 216-16
Recombinant murine IL-10	Peprotech	Cat# 210-10
DAPI	Solarbio	Cat# C0065
2,3,5-triphenyltetrazolium chloride	Sigma	Cat# T8877-5G
Critical commercial assays		
Cell Counting kit-8	TargetMol	C0005
LDH Cytotoxicity Assay Kit	Beyotime	C10017
ReverTra Ace® qPCR RT Master Mix with gDNA Remover	Toyobo	FSQ-301
Immobilon Western HRP substrate	Merck	WBKLS0500
Deposited data		
RNA-seq data	This paper	Accession number: PRJNA927235
Protein Mass Spectrometry data	This paper	Accession number: PXD040340
Experimental models: Cell lines		
Murine: Neuro-2a cell line	National Collection of Authenticated Cell Cultures	SCSP-5035
Experimental models: Organisms/strains		
Mouse: C57BL/6	Ji'nan Pengyue Laboratory Animal Breeding Co., Ltd	N/A
Oligonucleotides		
Primers in this paper, see Methods for RNA splicing and RIP analysis	This paper	N/A
Software and algorithms		
ImageJ	NIH	https://imagej.nih.gov/ij/
Prism	GraphPad	N/A
DAVID software	N/A	DAVID Functional Annotation Bioinformatics Microarray Analysis (ncifcrf.gov)

RESOURCE AVAILABILITY

Lead contact

Further information and requests for resources and reagents should be directed to and will be fulfilled by the lead contact: Qi Wan; e-mail: qiwan1@hotmail.com.

Materials avialibity

This study did not generate unique reagents.

Data and code availability

- RAN-seq data produced in this study are available at NCBI. The mass spectrometry proteomics data have been deposited to the ProteomeXchange Consortium (http://proteomecentral.proteomexchange.org) via the iProX partner repository. These data are publicly accessible as of the date of publication. Accessible numbers are listed in the key resources table.
- This study did not report orginal code.
- Any additional information required to reanalyze the data reported in this paper is available from the lead contact upon request.

EXPERIMENTAL MODEL AND STUDY PARTICIPANT DETAILS

Animals

Male 9-10 weeks C57BL/6 mice were all from Ji'nan Pengyue Laboratory Animal Breeding Co., Ltd. (China). The mice were housed at specific-pathogen-free (SPF) conditions at a constant temperature and humidity on a 12 h light/dark cycle. Food and water were given *ad libitum*. All animal experiments were conducted in compliance with National Institutes of Health guidelines and were approved by the institutional animal care and use committee of Qingdao University (20220401C5722520221220132). All the animal experiments conform to the ARRIVE guidelines.

Cell culture

The cortical neurons were prepared from the cortex of embryonic day 17 (E17) of C57BL/6 mice embryos.[45] The dissociated cortical neurons were suspended in a plating medium (Neurobasal medium, 2% B-27 supplement, 0.5% FBS, 0.5 mM L-glutamine and 25 mM glutamic acid) and plated on poly-D-lysine coated dishes. Half of the plating medium was removed and replaced with maintenance medium (Neurobasal medium, 2% B-27 supplement, and 0.5 μM L-glutamine) after 1 day in culture. From then on, the culture medium was changed every three days. After 11 days, the cultured neurons were used for further experiments.

The protocol of primary neonatal microglia cultures was adapted from the previous report.[45] The neonatal brain from 1 to 2 days mice were trypsinized and dissociated and cells were plated in a six-well plate in DMEM/Ham's F12 medium containing 10% FBS, penicillin and streptomycin. Culture media were changed every three days. Cells were allowed to reach 90% confluence. To harvest microglia, at day 9 *in vitro*, cultures were mildly trypsinized with trypsin solution (0.05% trypsin in DMEM/Ham's F12) at 37°C for 40 min. Floating cells were removed and the resulting enriched microglial cultures were trypsinized with 0.25% trypsin and plated for future experiments. The purity was over 95%.

Primary astrocytes culture

Astrocytes were prepared from the cortex of C57BL/6 mice at P0, as described previously.[46,47] The neonatal cortex was trypsinized (0.05% trypsin in DMEM/Ham's F12) and cells were plated at density in T75 tissue culture plates in DMEM medium containing 10% FBS. Culture media were changed three times a week. Cultures were shaken to remove the top layer of cells sitting over the astroglial monolayer to yield mainly astrocytes with a flat morphology between day 9 and 14.

Neuro-2a cell line were purchased from National Collection of Authenticated Cell Cultures (Shanghai, China). The cells were culture with DMEM medium containing 10% FBS. All cells were maintained at 37°C in a humidified incubator containing 5% CO2.

METHOD DETAILS

Focal cerebral ischemia

Suture occlusion technique was used to induce transient focal cerebral ischemia. Male 9-10 weeks C57BL/6 mice were anesthetized with 4% isoflurane in 70% N2O and 30% O2 with a mask. Make a midline incision in the neck, carefully expose and dissect the right external carotid artery (ECA), insert a diameter of about 0.22 mm monofilament nylon suture from the ECA into the left internal carotid artery and block the left middle cerebral artery (MCA). After occlusion for 60 minutes, the suture was removed for reperfusion, and ECA was ligated to close the wound. Sham-operated mice underwent the same surgery and/or intracerebroventricular injection except for immediate insertion and removal of sutures. Brain blood flow was measured in all mice animals using laser Doppler flowmetry (PERIMED PSI-Z). Animals that did not display a significant reduction in regional cerebral blood flow after ischemia were excluded from further experimentation. Mice were maintained on top of a warming pad (RWD, 69003) during the above procedures. The breathing machine was used to monitor the respiration of mice. The mice were returned to a heated cage during the recovery phase with free access to food and water. A total of 285 mcie were used for tMCAO analysis. Mice that showed no signs of neurological deficits during the acute phase after tMCAO or showed intracerebral hemorrhage during postmortem analysis were excluded from the study. To accurately assess the results, a first investigator administered the treatment based on the randomization table and were aware of the treatment group allocation. A second investigator was responsible for the anesthetic procedure, performed the surgical procedure and analyzed data.

TTC staining and neurological severity score analysis

We harvested the brain at 24 hr or 48 hr after tMCAO and performed TTC (2,3,5-triphenyltetrazolium chloride) staining. The brain was placed in a cooled matrix and cut into 1.2 mm coronal slices. The total six brain sections were placed in a 6 cm petri dish and incubated for 30 min at 37° C with 2% TTC in phosphate buffered saline (PBS). Sections were then fixed in 4% paraformaldehyde at 4°C. Viable brain tissue was stained red, whereas a pale gray color indicated infarcted tissue. All image acquisition, processing and analysis were performed blindly. Analyze the scanned image using image analysis software (Image-J).[45,48] Calculate infarct volume to correct for edema. The normal volume of the contralateral hemisphere and the normal volume of the ipsilateral hemisphere were measured and the percent infarction was calculated as % contralateral structure to avoid false positive secondary to edema.

Mice were tested for modifying neurological severity score (mNSS). Neurological deficits were tested using the following 9 points scale[45]: (1) absence of neurological deficits (0 points); (2) left forelimb flexion upon suspension by the tail or failure to fully extend the right forepaw (1 point); (3) left shoulder adduction upon suspension by the tail (2 points); (4) reduced resistance to a lateral push toward the left (3 points); (5) spontaneous movement in all directions, with circling to the left only if pulled by the tail (4 points); (6) circling or walking spontaneously only to the left (5 points); (7) walking only when stimulated (6 points); (8) no response to stimulation (7 points); and (9) stroke-related death (8 points).

Brain tissue sample preparation

The mice were transcardially perfused, the brains were immediately removed and then the olfactory bulbs were excised and the anterior and posterior brain tissue were cut into 1 mm sections. The remaining tissues of the ipsilateral (including the infarct and peri-infarct areas) and contralateral (normal) hemispheres were harvested and stored at -80°C.

RNA immunoprecipitation (RIP)

Neurons were harvested and lysed with lysis buffer (50mM Tris-HCl, pH 7.0, 150mM NaCl, 1mM MgCl2, 0.05% NP-40, 1mM phenylmethylsulfonyl fluoride, 10mM Ribonucleoside Vanadyl Complex) supplemented with 140Uml−1 of SUPERase·In (Thermo Fisher Scientific) and protease inhibitor cocktail. The clarified lysates were incubated with Anti-CHTOP antibody (Abcam) or IgG overnight at 4°C. Then 40 μl of protein A/G magnetic beads (Thermo Fisher Scientific) was added and incubated for 2 hr at 4°C. After four times washes using lysis buffer, the RNA on beads were extracted using TRIzol (Sigma) and qRT–PCR was performed. Primers: mouse Drd2 forward primer: 5′- TCTACGTGCCCT TCATCGTCACC -3′; reverse primer: 5′- GC TGGTGCTTGACAGCATCTCC -3′; Cdc14b forward primer: 5′- GATGAAGT CAG TGG AATGACACAAGGA-3′; reverse primer: 5′- GTTTAGTAATGCCTGCACTGC CAGA-3′. NTF3 forward primer: 5′- GAAGTCCTTCAAAGGGAT CGTTGG -3′; reverse primer: 5′- CAAGATGGACATCACCTTGTTCACC-3′. BDNF forward primer: 5′- GCTTTGGCAAAGCCATCCA CAC -3′; reverse primer: 5′-GCCCATTC ACGCTCTCCAGAGT -3′.

Neuron viability assays

CCK8 assay method

Cell survival was assayed by Cell Counting Kit-8 (TargetMol, USA), based on the manufacturer's instructions. Cortical neurons were plated at a density of 2×10^5 cells per well in 48-well plates. After virus transfection or indicated treatment, CCK-8 solution was added into each well, followed by incubation for 1–4 hr. Cell viability was determined by measuring the OD at 450 nm. Percent over control was calculated as a measure of cell viability.

LDH release method

LDH release was measured according to the manufacturer's instructions (Beyotime, China). Absorbance data were obtained at 490 nm to determine the LDH content. Absorbance data were obtained using a 96-well plate reader (Molecular Devices, USA) at 490 nm. LDH release (%) was calculated by calculating the ratio of experimental LDH release to maximum LDH release according to the manufacturer's instructions.

RNA extraction, reverse transcription and PCR for splicing analysis

The specific splicing primers used for splicing analysis are below: mouse Dlgap forward primer: 5′-CCTGCATCGGAAGCGTGGAA-3′; reverse primer: 5′- GGCTCAGCAGGTACGGCTTGT -3′; mouse Drd2 forward primer: 5′- TCTACGTG CCCTTCATCGTCACC -3′; reverse primer: 5′- GCTGGTGCTTGACAGCATCTCC -3′; mouse Gabra2 forward primer: forward primer: 5′- ACGTGACCAGTTTTGG CCCTGT-3′; reverse primer: 5′- GATTTAACC TGGAGCCATCGGG-3′; mouse Rnps1 forward primer: 5′- TGGTCTGAGAAGAGCGGGAGGA-3′; reverse primer:5′- GAGAAGG AGCCCTAGTGCTGGACT-3′; Lcmt1 forward primer: 5′- GTTTCAGCCAGTCCTCTTGGAATC-3′; reverse primer: 5′- ATTC TCCGAAG ACCACCATCAGG-3′; NcoR2 primer: 5′- ACACAGCCTCC TGGTGGAAGTTC-3′; reverse primer: 5′-GGCAGGAACGTGCGGG ACT-3′; Gmppa primer5′- AGTGGCA GGCGGCAGAGCT-3′; reverse primer: 5′- CGCCTGCCACAGGAAACAGA-3′; Cyb5R1 primer: 5′-CCTGAAGGAGGGAAGATGTCTCAAT -3′; reverse primer: 5′- TGTCCCACCAGCAATCATTCCC-3′; Cdc14b primer: 5′- GATGAAGTC AGTGG AATGACACA AGGA-3′; reverse primer: 5′- GTTTAGTAATGCCTGCACTGCCAG A-3′. NTF3 primer: 5′- GAAGTCCTTCAAAG GGATCGTTGG -3′; reverse primer: 5′- CAAGATGGACATCACCTTGTTCACC-3′. BDNF primer: 5′- GCTTTGGCAA AGCCATCCACAC -3′; reverse primer: 5′-GCCCATTCACGCTCTCCAGAGT -3′.

OGD treatment

For the OGD challenge, neurons were transferred to deoxygenated glucose-free extracellular solutions (in mM: 116 NaCl, 5.4 KCl, 0.8 MgSO4, 1.0 NaH2PO4, 1.8 CaCl2 and 26 NaHCO3); placed into the anaerobic incubator (CONCEPT400, RUSKIN, UK) and held in 95% N2/5% CO2 at 37°C for indicated times. The medium was then replaced with fresh maintenance medium containing the appropriate concentration of reagents for the indicated times during recovery in a 95% O2/5% CO2 incubator at 37°C.

Lentivirus *in vitro* infection methods

Lentivirus preparation

For CHTOP overexpression experiments, cDNAs of the mouse CHTOP gene were cloned into the Ubi-MCS-3FLAG-CBh-gcGFP-IRES -puromycinp retroviral vector (GeneChem Technology). To knockdown CHTOP, we used the siRNA sequence: GGAGCAGCTGGACAACCAA to construct the lentiviral vector (LV3 vector constructed from Genepharma Technology). The virus was packaged in the 293T cell line, and after transfection for 48 h, viral culture supernatants were harvested and concentrated.

In vitro infection

Primary cortical neurons were infected with the indicated lentivirus. Three days after the infection, infected neurons were used for further analysis.

Adeno-associated virus (AAV) *in vivo* administration methods

AAV preparation

For CHTOP overexpression experiments, cDNAs of the mouse CHTOP gene were cloned into the pAAV-hSyn-EGFP-P2A-3xFLAG-WPRE AAV vector. To knockdown CHTOP, we used the siRNA sequence: GGAGCAGCTGGACAACCAA to construct the AAV plasmid pAAV-hSyn-EGFP- 3xFLAG-miR30shRNA (Chtop) -WPRE. The indicated AAV virus was packaged and provided by Obio Technology Corp., Ltd.

In vivo administration

AAV was stereotaxically injected into the ischemic cortex at three sites on the left as follows: site 1, 0.3 mm anterior to bregma, lateral 3 mm to midline, 2 mm deep; site 2, 0.8 mm posterior to bregma, lateral 3 mm to midline, 2.2 mm deep; site 3, 1.9 mm posterior to bregma, lateral 3 mm to midline, 2.5 mm deep. Each site was injected with 1μL AAV for 5 minutes. After injection for 21 days, tMCAO was performed in the left side of the brain.

Behavior analysis

For the rotarod test, mice were trained twice daily (10 min per session) for three consecutive days at the speed of 10 rpm before tMCAO. For the formal test, mice were placed on a rotating drum with speeds starting at 4 rpm and accelerating to 45 rpm within 240s. Three times daily to assess overall coordination and balance. The Rota-Rod test apparatus was used (HUAYO-NHR420).

Immunoblot, Immunoprecipitation (IP) and Mass Spectrometry

Cells were lysed with 1× SDS lysis buffer and incubated at 100°C for 15 min. Proteins were separated by SDS-PAGE and transferred to nitrocellulose membranes (Millipore). Membranes were blocked with 5% milk or 5% BSA in Tris buffered saline and Tween 20 for 60 min at room temperature. Then the membranes were incubated with primary and secondary antibodies. Membranes were exposed and analyzed with a chemiluminescence detection system (Image Quant 800, Cytiva).

For immunoprecipitation, cells were lysed in lysis buffer (150 mM NaCl, 1% Triton X-100, 1 mM EDTA, and 50 mM Tris-HCl), supplemented with a protease inhibitor cocktail. Cell lysates were incubated with the primary antibody overnight. Protein A/G magnetic beads (Thermo) were added the next day for 2 hrs at 4°C. Antibody-Beads conjugates were washed four times with lysis buffer, and eluted with 1× SDS sample buffer. The eluates were subjected to immunoblot analysis or silver staining. For MS, the cut protein lanes were sequenced by BGI technology. Proteins identified from MS were listed in Table S1. Cellular component analysis was performed by using DAVID: Functional Annotation Tools (ncifcrf.gov).[49]

Immunofluorescence

Animals were perfused with 4% PFA, brains harvested, sectioned at 40μm and processed for immunofluorescence staining. The brain slices were fixed with 4% paraformaldehyde in PBS, perforated with 0.3% Triton X-100 for 30 min at room temperature and blocked with 10% indicated serums for 2 hr at room temperature. Cultured cells were fixed with 4% paraformaldehyde in PBS for 30 min, permeabilized and with 0.5% Triton X-100 for 30 min at room temperature and blocked with 5% BSA for 1hr at room temperature. Sections or cells were further incubated with primary antibodies overnight, washed three times with PBS the next day and incubated with secondary antibodies for 1 hr at room temperature. The nuclei were stained with DAPI (S2110, Solarbio). Slides were taken with a confocal microscope Nikon C2 and analyzed using ImageJ software. The following antibodies were used: rabbit anti-CHTOP (ab222861, Abcam, 1:2000), mouse anti-NeuN (MAB377, Millipore,1:500), mouse anti-GFAP (MAB360, Millipore, 1:1000), goat anti-Iba-1 (NB100-1028, Novus, 1:1000), mouse anti-RBM25 (sc-374271, Santa Cruz, 1:200), mouse anti-SC35 (67469-1-Ig, Proteintech, 1:1000), mouse anti-SF3B3 (67469-1-Ig, Proteintech, 1:1000), mouse anti-Prmt1(sc-166963, Santa Cruz,1:500), mouse anti-MAP2 (M4403, sigma,1:1000). Donkey anti-rabbit 488 (A21206), Donkey anti-mouse 568 (A10037), Donkey anti-goat 568 (A11057), Donkey anti-mouse 488 (A21202), Donkey anti-rabbit 548 (A10042) from Thermo Fisher Scientific.

RNA sequencing and data analysis

RNA was extracted and RNA integrity was assessed using the RNA Nano 6000 Assay Kit of the Bioanalyzer 2100 system (Agilent Technologies, CA, USA). RNA was enriched by Oligo (dT)-attached magnetic beads, followed by fragmentation and reverse transcription with random primers. Obtained cDNAs were purified their 5′ and 3′ ends were repaired and ligated with adapters. PCR products were purified (AMPure XP system) and library quality was assessed on the Agilent Bioanalyzer 2100 systems. The clustering of the index-coded samples was performed on a cBot Cluster Generation System using TruSeq PE Cluster Kit v3-cBot-HS (Illumia) according to the manufacturer's instructions. After cluster generation, the library preparations were sequenced on an Illumina Novaseq platform and 150 bp paired-end reads were generated.

We used clusterProfiler R package to test the statistical enrichment of differential expression genes in KEGG pathways (http://www.genome.jp/kegg/). For alternative splicing analysis, rMATS (v4.1.0) software was used to define alternative splicing levels of exon skipping, intron retention, mutually exclusive exon inclusions, alternative 5′ splice sites, and alternative 3′ splice sites as previously reported [31].

QUANTIFICATION AND STATISTICAL ANALYSIS

Statistical analysis

The statistical analysis was performed using GraphPad Prism software. All experiments were performed three or more times unless otherwise indicated. All data were shown as Mean ± S.D. To compare the statistical significance of two independent groups, Student's t-test (two-tailed) was used unless otherwise indicated. Differences between multiple groups were analyzed by one-way or two-way ANOVA followed by indicated test shown in the Figure legends. The detailed information were listed in the Figure legends.